Alternative oxidase alleviates mitochondrial oxidative stress during limited nitrate reduction in *Arabidopsis thaliana*

Daisuke Otomaru[a], Natsumi Ooi[a,b], Kota Monden[a], Takamasa Suzuki[c], Ko Noguchi[d], Tsuyoshi Nakagawa[a] and Takushi Hachiya[a†]

[a]Department of Molecular and Functional Genomics, Interdisciplinary Center for Science Research, Shimane University, 1060 Nishikawatsu-cho, Matsue, Shimane 690-8504, Japan

[b]Division of Biological Science, Nara Institute of Science and Technology, 8916-5 Takayama, Ikoma, Nara 630-0192, Japan

[c]College of Bioscience and Biotechnology, Chubu University, 1200 Matsumoto-cho, Kasugai, Aichi 487-8501, Japan

[d]Department of Life Sciences, Tokyo University of Pharmacy and Life Sciences, 1432-1 Horinouchi Hachioji, Tokyo 192-0392, Japan

[†]**To whom correspondence should be addressed.**

Takushi Hachiya

E-mail: takushi.hachiya@life.shimane-u.ac.jp

Tel.: +81-852-32-6288

Fax: +81-852-32-6109

Funding

This study was supported by KAKENHI Grants from the Japan Society for the Promotion of Science [Grant-in-Aid for Scientific Research (C) No. 20K05771/23K04978 to TH].

Abstract

The conversion of nitrate to ammonium, i.e., nitrate reduction, is a major consumer of reductants in plants. Previous studies have reported that the mitochondrial alternative oxidase (AOX) is upregulated under limited nitrate reduction conditions, including no/low nitrate or when ammonium is the sole nitrogen (N) source. Electron transfer from ubiquinone to AOX bypasses the proton-pumping complexes III and IV, thereby consuming reductants efficiently. Thus, upregulated AOX under limited nitrate reduction may dissipate excessive reductants and thereby attenuate oxidative stress. Nevertheless, so far there is no firm evidence for this hypothesis due to the lack of experimental systems to analyze the direct relationship between nitrate reduction and AOX. We therefore developed a novel culturing system for *A. thaliana* that manipulates activities of nitrate reduction and AOX separately without causing N starvation, ammonium toxicity, and lack of nitrate signal. Using this system we examined genome-wide gene expression and plant growth to better understand the relationship between AOX and nitrate reduction. Here we show that AOX alleviates mitochondrial oxidative stress and sustains plant growth under limited nitrate reduction.

53 **1 | INTRODUCTION**

54 Plants use nitrate and ammonium as main sources of nitrogen (N). The conversion of nitrate to
55 ammonium, i.e., nitrate reduction, requires eight moles of electrons per mole of nitrate, which
56 accounts for about half of the energy required for protein synthesis from nitrate (Hachiya et al.,
57 2007). Thus, ammonium is an energetically superior N source, but most crops prefer nitrate
58 (Miller & Cramer, 2004). In herbaceous plants, nitrate reduction generally occurs in the shoots
59 (Andrews et al., 1992; Hachiya et al., 2020; Scheurwater et al., 2002), and acts as a major sink of
60 reductants generated by the chloroplasts (Rasmusson et al., 2020). Hence, when the nitrate supply
61 is limited, excessive reductants may accumulate within illuminated photosynthetic cells. Recent
62 studies have shown that the NAD(P)H/NAD(P)$^+$ ratio and the levels of hydrogen peroxide are
63 increased in *A. thaliana* leaves of ammonium-grown plants compared with nitrate-grown plants
64 (Podgórska et al., 2013; Podgórska et al., 2020; Rasmusson et al, 2020). Moreover, N starvation
65 treatments have been found to enlarge the ascorbate pool in several plant species (Iwagami et al.,
66 2022). Taken together, these findings suggest that a decrease in nitrate reduction could lead to
67 oxidative stress in plants.

68 It is widely accepted that nitrate reduction significantly alters the action of the plant
69 mitochondrial electron transport chain (mETC) (Rasmusson et al., 2020). In fact, the amount of
70 electrons consumed in nitrate reduction appears to be comparable to that in the mETC (Noctor &
71 Foyer, 1998; Rasmusson et al., 2020). In photosynthetic tissues, the expression and activities of
72 several enzymes that bypass energy conservation steps in mETC are induced under limited nitrate
73 reduction conditions; i.e., if the plant is experiencing N starvation or if ammonium is the sole N
74 source (Escobar et al., 2006; Hachiya et al., 2010; Noguchi & Terashima, 2006; Qiao et al., 2022;
75 Watanabe et al., 2010). One enzyme is the alternative oxidase (AOX), which allows direct
76 electron transfer from ubiquinone to molecular oxygen, bypassing the proton-pumping complexes
77 III and IV (Noguchi & Yoshida, 2008). Therefore, upregulation of AOX under limited nitrate
78 reduction may dissipate excessive reductants without being limited to steep proton gradients

79 across the mitochondrial inner membrane, thereby attenuating reactive oxygen species (ROS)
80 production and oxidative stress. Actually, in *Arabidopsis* plants under low nitrate conditions, the
81 shoot expression of antioxidant enzyme genes was induced by disrupting the major isoform
82 *AOX1a* (Watanabe et al., 2010). Antisense suppression of *Arabidopsis AOX1a* was found to
83 greatly decrease the reducing state of ascorbate under ammonium but not under nitrate (Podgórska
84 et al., 2020). In barley grown under low nitrate, chemical inhibition of AOX activity elevated the
85 levels of hydrogen peroxide (Wang et al., 2016). Moreover, in tobacco cell cultures subjected to
86 N starvation, antisense suppression of *AOX1* caused carbohydrate accumulation (Sieger et al.,
87 2005). This implies that, under limited nitrate reduction, oxidation of NADH via AOX could
88 replenish the NAD^+ to drive the glycolysis.

89 The above studies suggest that AOX is linked to nitrate reduction. However, these
90 studies manipulated nitrate reduction activity by transferring plants to the growth conditions that
91 included no/low nitrate or the use of ammonium as the sole N source. Reduced nitrate reduction
92 may therefore be accompanied by N starvation or ammonium toxicity (Hachiya et al., 2021a),
93 causing plant growth suppression and/or the initiation of stress responses. Moreover, since nitrate
94 acts as a signal to alter genome-wide gene expression (Liu et al., 2017; Wang et al., 2004), a
95 decrease in the nitrate supply also depletes the nitrate signal. For these reasons, it is impossible
96 to distinguish whether the above-mentioned effects of AOX deficiency are caused by reduced
97 nitrate reduction, N starvation, ammonium toxicity, or the lack of nitrate signal. To solve this
98 problem, we developed a novel culturing system to manipulate the degree of nitrate reduction and
99 AOX activity without causing N starvation, ammonium toxicity, and the lack of nitrate signal.
100 Using this system we examined genome-wide gene expression and plant growth to better
101 understand the relationship between AOX and nitrate reduction.
102

103 **2 | MATERIALS AND METHODS**

104 2.1 Plant materials and growth conditions

105 In this study we used *A. thaliana*, accession Columbia (Col-0) as a control line as well as the
106 *aox1a-1* (SALK_084897, Giraud et al., 2008), *aox1a-2* (SAIL_030_D08, Giraud et al., 2008), *nr*
107 (*nia1-1/chl3-5*, Wang et al., 2004), *aox1a-1 nr*, and *aox1a-2 nr* mutants. The homozygous
108 multiple mutants of *aox1a-1 nr* and *aox1a-2 nr* were produced via crossing. The surface-sterilized
109 seeds were placed in the dark at 4°C for three days to break seed dormancy. For *in vitro* culturing,
110 we first grew plants on a sterile cellophane sheet (Hachiya et al., 2021b) placed on a solid medium
111 containing 30 mL half-strength Murashige and Skoog (1/2-MS) salts without nitrogen
112 supplemented with 2.5 mM $(NH_4)_2SO_4$, 0.1% (w/v) MES-KOH (pH 6.7), 0.5% (w/v) sucrose,
113 and 0.25% (w/v) gellan gum (Fujifilm Wako, Osaka, Japan). Plants were grown horizontally at
114 22°C for 18 days under a fixed photosynthetic photon flux density (PPFD) of 30 μmol m^{-2} s^{-1}
115 (i.e., constant light). Plants-on-cellophane were then transferred to a medium containing 30 mL
116 of 1/2-MS salts without nitrogen supplemented with 0.05% (w/v) MES-KOH (pH 5.7), 0.5%
117 (w/v) sucrose, and 0.25% (w/v) gellan gum (Fujifilm). The resulting mixture was incubated at
118 22°C for 24 h, also under a PPFD of 30 μmol m^{-2} s^{-1} (i.e., constant light). Finally, the plants-on-
119 cellophane were transferred to a medium containing 30 mL of 1/2-MS salts supplemented with
120 0.05% (w/v) MES-KOH (pH 5.7), 0.5% (w/v) sucrose, and 0.25% (w/v) gellan gum (Fujifilm)
121 and then incubated at 22°C under a PPFD of 150–200 μmol m^{-2} s^{-1} (constant light). For soil
122 cultivation, plants were grown for 14 or 24 days under a PPFD of 100–130 μmol m^{-2} s^{-1} (i.e., on
123 a 16h/8h light/dark cycle) at 22–23°C using an Arasystem 360 kit (Betatech BVBA, Gent,
124 Belgium) in a 1 : 1 mixture of nutrient-rich soil (Supermix A; Sakata Seed, Kyoto, Japan) and
125 vermiculite.
126
127 2.2 Determination of in vitro nitrate reductase activities
128 First, we assessed *in vitro* nitrate reductase (NR) activity using a previously published method
129 (Hachiya et al., 2016) with slight modification. Frozen samples were first ground in a Multi-Bead
130 Shocker (Yasui Kikai, Osaka, Japan) using zirconia beads. The resulting powder was then mixed

131 with 10 vol. of extraction buffer (50 mM HEPES-KOH, pH 7.6, 1 mM EDTA, 7 mM cysteine)
132 and the extracts were centrifuged at 20,400×g at 4°C for 10 min. Next, a 30 µl aliquot of the
133 supernatant was added to 90 µl of assay buffer (50 mM HEPES-KOH, pH 7.6, 133 µM NADH,
134 2 mM EDTA, 6.67 mM KNO_3). After incubation at 30°C for 2 and 17 min, 24 µl of 1% (w/v)
135 sulfanilamide solution in 1 N HCl and 24 µl of 0.02% (w/v) *N*-(1-naphthyl)ethylenediamine
136 dihydrochloride solution were added to 48 µl aliquots of reaction mixture. Finally, nitrite content
137 was determined based on absorbance readings at 540 nm. *In vitro* NR activity was calculated by
138 determining the nitrite amount produced over a 15 min period.
139
140 2.3 Determination of in vivo nitrate reductase activities
141 First, we submerged fresh shoots in 50 vols. of reaction buffer (i.e., 100 mM sodium phosphate
142 buffer, pH 7.4, 10 mM KNO_3, 4% (v/v) n-propanol), followed by vacuum-infiltration. The
143 reaction mixture was then incubated at 30˚C for 1 h in the dark. The amount of nitrate produced
144 was then visualized by mixing the supernatant with 1% (w/v) sulfanilamide solution in 1 N HCl,
145 and 0.02% (w/v) *N*-(1-naphthyl)ethylenediamine dihydrochloride solution in a 2 : 1 : 1 ratio.
146
147 2.4 Determination of nitrate concentration
148 Nitrate content was quantified as per a previously published protocol (Hachiya et al., 2016) with
149 slight modifications. Nitrate was first extracted with 10 vol. of deionized water at 100°C for 20
150 min. Next, 10 µL of the supernatant was mixed with 40 µL of a reaction reagent (i.e., 5% (w/v)
151 salicylic acid in concentrated sulfuric acid), and the resulting mixture was then incubated at room
152 temperature for 20 min. A mock treatment of 40 µL of concentrated sulfuric acid was also
153 produced. Finally, 1 mL of 8% (w/v) NaOH solution was added to the mixture, and nitrate was
154 determined based on absorbance at 410 nm.
155
156 2.5 Determination of total protein

157 Total protein was determined according to a previously described method (Hachiya et al., 2016).
158 Frozen samples were first homogenized with a Multi-Beads Shocker (Yasui Kikai) using zirconia
159 beads. Total proteins were then extracted with 10 vol. of sample buffer [2% (w/v) SDS, 62.5 mM
160 Tris-HCl (pH 6.8), 10% (v/v) glycerol, and 0.0125% (w/v) bromophenol blue] and Halt™
161 protease inhibitor cocktail (ThermoFisher Scientific, Tokyo, Japan), followed by incubation at
162 95°C for 5 min. Extracts were then centrifuged at 20,400×g at 8°C for 10 min and 10 μL aliquots
163 were suspended in 500 μL deionized water. Next, 100 μL 0.15% (w/v) sodium deoxycholate was
164 added, and the mixture was incubated at room temperature for 10 min. 100 μL of 72% (v/v)
165 trichloroacetic acid was then added, followed by incubation at room temperature for 15 min and
166 centrifugation at 20,400×g for 10 min. Precipitates were then air-dried and suspended in 25 μL
167 water. This suspension was used to determine total protein concentrations using Takara BCA
168 Protein Assay Kits (TaKaRa, Kusatsu, Japan).
169
170 2.6 Immunodetection of AOX and ACTIN proteins
171 12.35 μL of total protein extract was mixed with 0.65 μl of 1 M DTT, followed by incubation at
172 95˚C for 3 min. 5 μL of mixture (~0.43 mg fresh weight) was then subjected to SDS-PAGE using
173 a 12% Mini-PROTEAN TGX Gel (Bio-Rad, Hercules, CA, USA) before transferring to a Trans-
174 Blot Turbo Mini PVDF membrane using the Trans-Blot Turbo Transfer System (Bio-Rad).
175 Membranes were incubated for 1h in blocking buffer (50 mM Tris-HCl, and 150 mM NaCl, pH
176 7.6, 0.1% (v/v) Tween-20) containing 5% (w/v) ECL Prime Blocking Agent (Cytiva, Tokyo,
177 Japan). Membranes were then incubated for 1h with a 1/200 dilution of monoclonal antibodies
178 against AOX (AS10 699, Agrisera, Vännäs, Sweden) or a 1/2,500 dilution of polyclonal
179 antibodies against ACTIN (AS13 2640, Agrisera). Finally, the antigen–antibody complex was
180 detected using a 1/10,000 dilution of horseradish peroxidase conjugated with anti-mouse IgG
181 sheep antibodies (Cytiva) for AOX or anti-rabbit IgG donkey antibodies (Cytiva) for ACTIN by
182 ECL Prime chemiluminescent detection (Cytiva). Proteins blotted on membranes were visualized

183 using TaKaRa CBB Protein Safe Stain (TaKaRa) and chemiluminescence and CBB staining were
184 visualized using ImageQuant LAS 500 mini (Cytiva).
185
186 2.7 RNA extraction
187 Samples were first homogenized as described above. Next, total RNA was extracted using an
188 RNeasy Plant Mini Kit (Qiagen, Tokyo, Japan). For RNA-seq library preparation, RNA was
189 purified using on-column DNase digestion (Qiagen).
190
191 2.8 RNA-seq
192 RNA quality was first evaluated using a Qubit RNA IQ Assay Kit (ThermoFisher Scientific).
193 RNA samples with RNA IQs 8.7–10.0 were used for library preparation. cDNA libraries were
194 constructed using a NEBNext Ultra II RNA Library Prep Kit with Sample Purification Beads
195 (New England Biolabs, Tokyo, Japan), a NEBNext Poly(A) mRNA Magnetic Isolation Module
196 (New England Biolabs), and NEBNext Multiplex Oligos for Illumina (New England Biolabs).
197 cDNA libraries were then sequenced using a NextSeq 500 (Illumina, Tokyo, Japan), and resulting
198 bcl files were converted to fastq files using bcl2fastq (Illumina). The RNA-seq raw data are
199 available in ArrayExpress database under accession number E-MTAB-14027. Finally, obtained
200 reads were analyzed using iDEP version 096 (Ge et al., 2018), Metascape (Zhou et al., 2019), and
201 GeneCloud (Krouk et al., 2015) using the default settings.
202
203 2.9 RT-qPCR
204 Reverse transcription (RT) was performed using a ReverTraAce qPCR RT Master Mix with
205 gDNA Remover (Toyobo, Osaka Japan). Synthesized cDNA was then diluted tenfold with water
206 and used for quantitative PCR (qPCR). RT-qPCR was performed on a QuantStudio 1
207 (ThermoFisher Scientific) with KOD SYBR qPCR Mix (Toyobo). Relative transcript levels were
208 calculated using the comparative cycle threshold method with *ACTIN3* as an internal standard.

209 Primer sequences are shown in Table S1.

210

211 2.10. Statistical analysis

212 The Tukey–Kramer multiple comparison test were conducted using R software v.2.15.3.

213

214 **3 | RESULTS and DISCUSSION**

215 3.1 Manipulation of nitrate reduction and AOX activities

216 We manipulated the activities of nitrate reduction and AOX via the transfer experiment (Figure
217 1A) using Col-0 and the mutants deficient in either or both of NR and AOX activities. First, plants
218 were grown for 18 days with ammonium as the sole N source to ensure uniform growth
219 independently of NR activity. Higher medium pH and lower light intensity were used to reduce
220 ammonium toxicity and AOX expression (Escobar et al., 2006; Hachiya et al., 2010; Hachiya et
221 al., 2021a; Yoshida et al., 2011), allowing uniform growth regardless of AOX activity. Second,
222 plants were subjected to N starvation at pH 5.7 for 24 h to induce AOX expression (Escobar et
223 al., 2006; Hachiya et al., 2010). Finally, plants were transferred to a medium containing adequate
224 nitrate and incubated at an elevated light intensity, which induces NR expression and fills
225 photosynthetically-derived reductants to the cell (Noguchi & Yoshida, 2008; Wang et al., 2004;
226 Yoshida et al., 2010). The NR activity of Col-0 increased rapidly from 0 to 7 h after nitrate supply
227 and slightly more from 7 to 24 h (Figure S1A). Both *in vitro* and *in vivo* NR activities were
228 increased 7 h after nitrate supply in the shoots of Col-0 and *aox1a-1*, but not in *nr* and *aox1a-1*
229 *nr* (Figures 1B and 1C). Thus, we focused on the 7 h after nitrate supply to identify the early
230 effects of nitrate reduction for subsequent experiments. We found that nitrate accumulated in the
231 shoots of all lines after nitrate supply, with concentrations ranging from 14.7 to 21.6 μmol g^{-1}
232 (Figure 1D), indicating an adequate supply of nitrate for signaling. Actually, expression of *NIA2*
233 encoding the major NR isoform in leaves, which is inducible by nitrate signal (Konishi &
234 Yanagisawa, 2013; Wilkinson & Crawford, 1991), was strongly induced 7 h after nitrate supply

235 (Figure S1B). Higher nitrate concentrations in shoots of *nr* and *aox1a-1 nr* than Col-0 and *aox1a-*
236 *1* would reflect a deficiency in nitrate reduction (Figure 1D). Shoot protein concentrations were
237 comparable among all lines before and after nitrate supply, ranging from 27.0 to 29.7 mg g^{-1}
238 (Figure 1E), suggesting that no N starvation occurred. RT-qPCR and Western blot analyses
239 confirmed that the signals corresponding to *AOX1a* and AOX were negligible in *aox1a-1* and
240 *aox1a-1 nr* (Figures S1C and S1D), suggesting that knockout of *AOX1a* is sufficient to diminish
241 AOX activity, as reported earlier (Giraud et al., 2008; Hachiya et al., 2010). Taken together, these
242 culturing conditions permit comparisons of plants differing nitrate reduction and AOX activity
243 without causing ammonium toxicity, N starvation, and lack of nitrate signaling.

244 3.2 AOX alleviates mitochondrial oxidative stress under limited nitrate reduction

245 Next, to dissect the role of AOX in limited nitrate reduction, we performed three independent
246 RNA-seq analyses using shoots from Col-0, *aox1a-1*, *aox1a-2*, *nr*, *aox1a-1 nr*, and *aox1a-2 nr* 7
247 h after nitrate supply (Table S2). A k-means clustering analysis classified transcripts into four
248 groups according to their expression patterns (Figure 2A and Table S3). In cluster D, *AOX1a*
249 deficiency consistently induced gene expression in the *nr* background, but not in the Col-0
250 background (Figures 2A and 2B). Moreover, 42 of 141 genes in cluster D were statistically
251 significantly upregulated in *aox1a-1 nr* and *aox1a-2 nr* relative to *nr* (Figure 2C and Table S4).
252 Further enrichment analyses of the 42 genes identified significant overrepresentation of the terms
253 "toxin catabolic process," "glutathione metabolism" (Figure 2D), "interpro-ipr004046
254 (glutathione S-transferase, C-terminal)," and "gst" (Figure 2E). These terms were derived from
255 the glutathione S-transferase (GST) genes *AT2G29460* (*GSTU4*), *AT1G17170* (*GSTU24*),
256 *AT1G17180* (*GSTU25*), and *AT1G02920* (*GSTF7*) (Table S4). *GSTU4*, a plant-specific tau class
257 GST, may contribute to hydrogen peroxide degradation by using glutathione as an electron donor
258 (Santamaría et al., 2018). The terms "response to hypoxia" and "response to oxidative stress"
259 were also enriched in these 42 genes (Figure 2D). Furthermore, genes induced by hypoxia
260 (Tamura & Bono, 2022) and H_2O_2 treatments (Hieno et al., 2019) were significantly upregulated

261 in *nr*, and their induction was enhanced by *AOX1a* deficiency (Figures 2F and 2G and Tables S5
262 and S6). The NAC transcription factor ANAC017 mediates ROS-related mitochondrial retrograde
263 signaling, thereby activating mitochondrial dysfunction stimulation genes including *AOX1a*,
264 *UPOX*, and *ANAC013* (De Clercq et al., 2013; Ng et al., 2013). The expression of ANAC017-
265 inducible genes (Ng et al., 2013) and mitochondrial dysfunction stimulation genes (De Clercq et
266 al., 2013) reached a maximum level in *aox1a nr and aox1a-2 nr* (Figures 2H and 2I and Tables
267 S7 and S8). Further RT-qPCR analyses revealed that the expression levels of hypoxia-inducible
268 genes (Figures 2J–M) and oxidative stress marker genes (Figures 2N–Q) were induced by nitrate
269 supply in *nr*, and this induction was enhanced by *AOX1a* deficiency. Meanwhile, before nitrate
270 supply, little difference was observed among all lines (Figures 2J–Q). Since hypoxia elevates
271 intracellular NADH/NAD^+ ratio via mETC inhibition (Igamberdiev et al., 2005), the upregulation
272 of hypoxia-inducible genes may reflect reductant accumulation. Consequently, our transcriptome
273 analysis suggests that AOX dissipates excessive reductants and mitigate oxidative stress under
274 limited nitrate reduction.

275 The plant mETC possesses type II NAD(P)H dehydrogenases located on the cytosol
276 side (ND_{ex}) or matrix side (ND_{in}) of the inner mitochondrial membrane (Rasmusson et al., 2020).
277 Since these dehydrogenases transfer electrons to ubiquinone and bypass the proton-pumping
278 complex I, they can dissipate excessive reductants like AOX. Of these, the expression of *NDB2*,
279 encoding the primary ND_{ex} contributor to NADH oxidation, was significantly induced in *nr* after
280 nitrate supply, and this induction was intensified by *AOX1a* deficiency (Figures 3A and 3B). Since
281 cytosolic NR has a much lower K_m for NADH than ND_{ex} (Sweetman et al., 2019), NDB2 may
282 operate only when nitrate reduction is limited. The *NDA2*, encoding the NADH-oxidizing ND_{in}
283 (Rasmusson et al., 2020), also showed a expression pattern similar to *NDB2* after nitrate supply
284 (Fig. 3A and 3C). The compensated induction of *NDB2* and *NDA2* by *AOX1a* deficiency (Figures
285 3) suggests a contribution of AOX1a-NDB2 and AOX1a-NDA2 modules to balance cellular
286 redox under limited nitrate reduction. Also, the STRING database ver. 12.0 integrating protein-

287 protein interactions (Szklarczyk et al., 2023) confirmed tight functional connections between
288 AOX1a, NDB2, and NDA2. Meanwhile, the expression of the uncoupling proteins (UCPs), which
289 act as an uncoupler and/or as an aspartate/glutamate exchanger across the inner mitochondrial
290 membrane (Monné et al., 2018), was little changed among the lines (Figure 3A).
291
292 3.3 AOX sustains plant growth under limited nitrate reduction
293 Finally, we analyzed shoot growth parameters following nitrate supply. Over 6 days, we found
294 that *AOX1a* deficiency significantly reduced (−15%) shoot fresh weight in *nr*, but not in Col-0
295 (Figure 4A). Meanwhile, rosette diameter was little affected by *AOX1a* deficiency (Figure 4B).
296 When plants were grown in nutrient-rich soil, shoot appearance and shoot fresh weight were
297 decreased in *aox1a-1 nr* and *aox1a-2 nr* relative to the others (Figures 4C–E). However, in NR-
298 deficient plants, leaves were pale green (Figure 4C). Thus, it is plausible that long-term limitation
299 of nitrate reduction could cause N starvation, which complicates the interpretation of the
300 relationship between nitrate reduction, AOX, and shoot growth.
301
302 **4 | CONCLUSIONS**
303 We have successfully developed a cultural system to manipulate activities of nitrate reduction
304 and AOX without causing ammonium toxicity, N starvation, and lack of nitrate signaling.
305 Analyses using this system suggest that AOX alleviates mitochondrial oxidative stress and sustain
306 plant growth under limited nitrate reduction. It awaits further analyses to address physiological
307 and biochemical details using the system based on knowledge obtained from the present study.
308
309 **AUTHOR CONTRIBUTIONS**
310 DO and NO performed most of the measurements and downstream analyses. KM supported most
311 of the measurements and downstream analyses. TS performed next-generation sequencing
312 analysis. KN and TN supervised all analyses and interpretations. TH designed the study,

313 performed a part of growth analysis, and supervised all analyses and interpretations. All authors
314 contributed to the writing and/or reviewing of the manuscript.
315
316 **ACKNOWLEDGEMENTS**
317 *aox1a-2* seeds were provided by Dr. James Whelan (La Trobe University, Australia). The authors
318 thank Enago for English language review.
319
320
321 **DATA AVAILABILITY STATEMENT**
322 The RNA-seq raw data are available in ArrayExpress under accession number E-MTAB-14027
323 (https://www.ebi.ac.uk/biostudies/arrayexpress).
324
325 **REFERENCES**
326 Andrews, M., Morton, J. D., Lieffering, M., Bisset, L., 1992. The partitioning of nitrate
327 assimilation between root and shoot of a range of temperate cereals and pasture grasses. *Ann. Bot.*
328 70(3), 271–276. https://doi.org/10.1093/oxfordjournals.aob.a088469
329
330 De Clercq, I., Vermeirssen, V., Van Aken, O., Vandepoele, K., Murcha, M. W., Law, S. R., Inzé,
331 A., Ng, S., Ivanova, A., Rombaut, D., van de Cotte, B., Jaspers, P., Van de Peer, Y., Kangasjärvi,
332 J., Whelan, J., Van Breusegem, F., 2013. The membrane-bound NAC transcription factor
333 ANAC013 functions in mitochondrial retrograde regulation of the oxidative stress response in
334 *Arabidopsis*. *Plant Cell* 25(9), 3472–3490. https://doi.org/10.1105/tpc.113.117168
335
336 Escobar, M. A., Geisler, D. A., Rasmusson, A. G., 2006. Reorganization of the alternative
337 pathways of the Arabidopsis respiratory chain by nitrogen supply: opposing effects of ammonium

338 and nitrate. *Plant J.* 45(5), 775–788. https://doi.org/10.1111/j.1365-313X.2005.02640.x
339
340 Ge, S. X., Son, E. W., Yao, R., 2018. iDEP: an integrated web application for differential
341 expression and pathway analysis of RNA-Seq data. *BMC Bioinform.* 19, 534.
342 https://doi.org/10.1186/s12859-018-2486-6
343
344 Giraud, E., Ho, L. H. M., Clifton, R., Carroll, A., Estavillo, G., Tan, Y. F., Howell, K. A., Ivanova,
345 A., Pogson, B. J., Millar, A. H., Whelan, J., 2008. The absence of ALTERNATIVE OXIDASE1a
346 in Arabidopsis results in acute sensitivity to combined light and drought stress. *Plant Physiol.*
347 147(2), 595–610. https://doi.org/10.1104/pp.107.115121
348
349 Hachiya, T., Terashima, I., Noguchi, K., 2007. Increase in respiratory cost at high growth
350 temperature is attributed to high protein turnover cost in *Petunia* × *hybrida* petals. *Plant Cell*
351 *Environ.* 30(10), 1269–1283. https://doi.org/10.1111/j.1365-3040.2007.01701.x
352
353 Hachiya, T., Watanabe, C. K., Boom, C., Tholen, D., Takahara, K., Kawai-Yamada, M.,
354 Uchimiya, H., Uesono, Y., Terashima, I., Noguchi, K., 2010. Ammonium-dependent respiratory
355 increase is dependent on the cytochrome pathway in *Arabidopsis thaliana* shoots. *Plant Cell*
356 *Environ.* 33(11), 1888–1897. https://doi.org/10.1111/j.1365-3040.2010.02189.x
357
358 Hachiya, T., Ueda, N., Kitagawa, M., Hanke, G., Suzuki, A., Hase, T., Sakakibara, H., 2016.
359 Arabidopsis root-type ferredoxin:NADP(H) oxidoreductase 2 is involved in detoxification of
360 nitrite in roots. *Plant Cell Physiol.* 57(11), 2440–2450. https://doi.org/10.1093/pcp/pcw158
361
362 Hachiya, T., Okamoto, Y., Watanabe, M.. Takebayashi, Y., Kojima, M., Suzuki, T., Sakakibara,
363 H., 2020. Genome-wide responses to shoot nitrate satiety are attenuated by external ammonium

364 in *Arabidopsis thaliana*. *Soil Sci. Plant Nutr.* 66(2), 317–327.
365 https://doi.org/10.1080/00380768.2020.1717905
366
367 Hachiya, T., Inaba, J., Wakazaki, M., Sato, M., Toyooka, K., Miyagi, A., Kawai-Yamada, M.,
368 Sugiura, D., Nakagawa, T., Kiba, T., Gojon, A., Sakakibara, H., 2021a. Excessive ammonium
369 assimilation by plastidic glutamine synthetase causes ammonium toxicity in *Arabidopsis thaliana*.
370 *Nat. Commun.* 12(1), 4944. https://doi.org/10.1038/s41467-021-25238-7
371
372 Hachiya, T., Oya, T., Monden, K., Nagae, A., Nakagawa, T., 2021b. A cellophane-supported
373 *Arabidopsis* culture for seamless transfer between different media is useful for studying various
374 nitrogen responses. *Soil Sci. Plant Nutr.* 67(3), 277–282.
375 https://doi.org/10.1080/00380768.2021.1908094
376
377 Hieno, A., Naznin, H. A., Inaba-Hasegawa, K., Yokogawa, T., Hayami, N., Nomoto, M., Tada,
378 Y., Yokogawa, T., Higuchi-Takeuchi, M., Hanada, K., Matsui, M., Ikeda, Y., Hojo, Y., Hirayama,
379 T., Kusunoki, K., Koyama, H., Mitsuda, N., Yamamoto, Y. Y., 2019. Transcriptome analysis and
380 identification of a transcriptional regulatory network in the response to H_2O_2. *Plant Physiol.*
381 180(3), 1629–1646. https://doi.org/10.1104/pp.18.01426
382
383 Igamberdiev, A. U., Baron, K., Manac'h-little, N., Stoimenova, M., Hill, R. D., 2005. The
384 haemoglobin/nitric oxide cycle: involvement in flooding stress and effects on hormone signalling.
385 *Ann. Bot.* 96(4), 557–564. https://doi.org/10.1093/aob/mci210
386
387 Iwagami, T., Ogawa, T., Ishikawa, T., Maruta, T., 2022. Activation of ascorbate metabolism by
388 nitrogen starvation and its physiological impacts in *Arabidopsis thaliana*. *Biosci. Biotech.*
389 *Biochem.* 86(4), 476–489. https://doi.org/10.1093/bbb/zbac010

390

391 Konishi, M., Yanagisawa, S., 2013. Arabidopsis NIN-like transcription factors have a central role
392 in nitrate signalling. *Nat. Commun.* 4(1), 1617. https://doi.org/10.1038/ncomms2621
393

394 Krouk, G., Carré, C., Fizames, C., Gojon, A., Ruffel, S., Lacombe, B., 2015. GeneCloud reveals
395 semantic enrichment in lists of gene descriptions. *Mol. Plant* 8(6), 971–973.
396 https://doi.org/10.1016/j.molp.2015.02.005
397

398 Miller, A. J., Cramer, M. D., 2004. Root nitrogen acquisition and assimilation. *Plant Soil* 274, 1–
399 36. https://doi.org/10.1007/s11104-004-0965-1
400

401 Monné, M., Daddabbo, L., Gagneul, D., Obata, T., Hielscher, B., Palmieri, L., Miniero, D. V.,
402 Fernie, A. R., Weber, A. P. M., Palmieri, F., 2018. Uncoupling proteins 1 and 2 (UCP1 and UCP2)
403 from *Arabidopsis thaliana* are mitochondrial transporters of aspartate, glutamate, and
404 dicarboxylates. *J. Biol. Chem.* 293(11), 4213-4227. https://doi.org/10.1074/jbc.RA117.000771
405

406 Ng, S., Ivanova, A., Duncan, O., Law, S. R., Van Aken, O., De Clercq, I., Wang, Y., Carrie, C.,
407 Xu, L., Kmiec, B., Walker, H., Van Breusegem, F., Whelan, J., Giraud, E., 2013. A membrane-
408 bound NAC transcription factor, ANAC017, mediates mitochondrial retrograde signaling in
409 *Arabidopsis*. *Plant Cell* 25(9), 3450–3471. https://doi.org/10.1105/tpc.113.113985
410

411 Noctor, G., Foyer, C. H., 1998. A re-evaluation of the ATP : NADPH budget during C_3
412 photosynthesis: a contribution from nitrate assimilation and its associated respiratory activity?. *J.*
413 *Exp. Bot.* 49(329), 1895–1908. https://doi.org/10.1093/jxb/49.329.1895
414

Noguchi, K., Terashima, I., 2006. Responses of spinach leaf mitochondria to low N availability. *Plant Cell Environ.* 29(4), 710–719. https://doi.org/10.1111/j.1365-3040.2005.01457.x

Noguchi, K., Yoshida, K., 2008. Interaction between photosynthesis and respiration in illuminated leaves. *Mitochondrion* 8(1), 87–99. https://doi.org/10.1016/j.mito.2007.09.003

Podgórska, A., Gieczewska, K. Łukawska-Kuźma, K., Rasmusson, A. G., Gardeström, P., Szal, B., 2013. Long-term ammonium nutrition of *Arabidopsis* increases the extrachloroplastic NAD(P)H/NAD(P)$^+$ ratio and mitochondrial reactive oxygen species level in leaves but does not impair photosynthetic capacity. *Plant Cell Environ.* 36(11), 2034–2045. https://doi.org/10.1111/pce.12113

Podgórska, A., Mazur, R., Ostaszewska-Bugajska, M., Kryzheuskaya, K., Dziewit, K., Borysiuk, K., Wdowiak, A., Burian, M., Rasmusson, A. G., Szal, B., 2020. Efficient photosynthetic functioning of *Arabidopsis thaliana* through electron dissipation in chloroplasts and electron export to mitochondria under ammonium nutrition. *Front. Plant Sci.* 11, 103. https://doi.org/10.3389/fpls.2020.00103

Qiao, X., Ruan, M., Yu, T., Cui, C., Chen, C., Zhu, Y., Li, F., Wang, S., Na, X., Wang, X., Bi, Y., 2022. UCP1 and AOX1a contribute to regulation of carbon and nitrogen metabolism and yield in Arabidopsis under low nitrogen stress. *Cell. Mol. Life Sci.* 79, 69. https://doi.org/10.1007/s00018-021-04036-w

Rasmusson, A. G., Escobar, M. A., Hao, M., Podgórska, A., Szal, B., 2020. Mitochondrial NAD(P)H oxidation pathways and nitrate/ammonium redox balancing in plants. *Mitochondrion* 53, 158–165. https://doi.org/10.1016/j.mito.2020.05.010

Santamaría, M. E., Arnaiz, A., Velasco-Arroyo, B., Grbic, V., Diaz, I., Martinez, M., 2018. Arabidopsis response to the spider mite *Tetranychus urticae* depends on the regulation of reactive oxygen species homeostasis. *Sci. Rep.* 8(1), 9432. https://doi.org/10.1038/s41598-018-27904-1

Scheurwater, I., Koren, M., Lambers, H., Atkin, O. K., 2002. The contribution of roots and shoots to whole plant nitrate reduction in fast- and slow-growing grass species. *J. Exp. Bot.* 53(374), 1635–1642. https://doi.org/10.1093/jxb/erf008

Sieger, S. M., Kristensen, B. K., Robson, C. A., Amirsadeghi, S., Eng, E. W. Y., Abdel-Mesih, A., Møller, I. M., Vanlerberghe, G. C., 2005. The role of alternative oxidase in modulating carbon use efficiency and growth during macronutrient stress in tobacco cells. *J. Exp. Bot.* 56(416), 1499–1515. https://doi.org/10.1093/jxb/eri146

Sweetman, C., Waterman, C. D., Rainbird, B. M., Smith, P. M. C., Jenkins, C. D., Day, D. A., Soole, K. L., 2019. AtNDB2 is the main external NADH dehydrogenase in mitochondria and is important for tolerance to environmental stress. *Plant Physiol.* 181(2), 774-788. https://doi.org/10.1104/pp.19.00877

Szklarczyk, D., Kirsch, R., Koutrouli, M., Nastou, K., Mehryary, F., Hachilif, R., Gable, A. L., Fang, T., Doncheva, N. T., Pyysalo, S., Bork, P., Jensen, L. J., von Mering, C., 2023. The STRING database in 2023: protein–protein association networks and functional enrichment analyses for any sequenced genome of interest. *Nucleic Acids Res.* 51(D1), D638-D646. https://doi.org/10.1093/nar/gkac1000

Tamura, K., Bono, H., 2022. Meta-Analysis of RNA sequencing data of Arabidopsis and Rice

467 under hypoxia. *Life* 12(7), 1079. https://doi.org/10.3390/life12071079
468
469 Wang, F., Wang, X., Zhao, C., Wang, J., Li, P., Dou, Y., Bi, Y., 2016. Alternative pathway is
470 involved in the tolerance of highland barley to the low-nitrogen stress by maintaining the cellular
471 redox homeostasis. *Plant Cell Rep.* 35, 317–328. https://doi.org/10.1007/s00299-015-1886-6
472
473 Wang, R., Tischner, R., Gutiérrez, R. A., Hoffman, M., Xing, X., Chen, M., Coruzzi, G.,
474 Crawford, N. M., 2004. Genomic analysis of the nitrate response using a nitrate reductase-null
475 mutant of Arabidopsis. *Plant Physiol.* 136(1), 2512–2522. https://doi.org/10.1104/pp.104.044610
476
477 Watanabe, C. K., Hachiya, T., Takahara, K., Kawai-Yamada, M., Uchimiya, H., Uesono, Y.,
478 Terashima, I., Noguchi, K., 2010. Effects of AOX1a deficiency on plant growth, gene expression
479 of respiratory components and metabolic profile under low-nitrogen stress in *Arabidopsis*
480 *thaliana*. *Plant Cell Physiol.* 51(5), 810–822. https://doi.org/10.1093/pcp/pcq033
481
482 Wilkinson, J. Q., Crawford, N. M., 1991. Identification of the *Arabidopsis CHL3* gene as the
483 nitrate reductase structural gene *NIA2*. *Plant Cell* 3(5), 461-471.
484 https://doi.org/10.1105/tpc.3.5.461
485
486 Yoshida, K., Shibata, M., Terashima, I., Noguchi, K., 2010. Simultaneous determination of in
487 vivo plastoquinone and ubiquinone redox states by HPLC-based analysis. *Plant Cell Physiol.*
488 51(5), 836–841. https://doi.org/10.1093/pcp/pcq044
489
490 Yoshida, K., Watanabe, C. K., Hachiya, T., Tholen, D., Shibata, M., Terashima, I., Noguchi, Ko.,
491 2011. Distinct responses of the mitochondrial respiratory chain to long- and short-term high-light

environments in *Arabidopsis thaliana*. *Plant Cell Environ*. 34(4), 618–628. https://doi.org/10.1111/j.1365-3040.2010.02267.x

Zhou, Y., Zhou, B., Pache, L., Chang, M., Khodabakhshi, A. H., Tanaseichuk, O., Benner, C., Chanda, S. K., 2019. Metascape provides a biologist-oriented resource for the analysis of systems-level datasets. *Nat. Commun.* 10(1), 1523. https://doi.org/10.1038/s41467-019-09234-6

SUPPORTING INFORMATION

Additional supporting information can be found online in the Supporting Information section at the end of this article.

FIGURE LEGENDS

FIGURE 1 Manipulation of activities of nitrate reduction and AOX without causing N starvation, ammonium toxicity, and the lack of nitrate signal.

(A) Schematic diagram of experiment. (B-E) *in vitro* NR activity (B), *in vivo* NR activity (C), nitrate concentration (D), and total protein concentration (E) in plant shoots before and 7 h after nitrate supply. Two plants of each line (eight in total) per plate were grown, and two shoots were pooled as one biological replicate. Data: mean ± SD (n = 3 (B), n = 5–9 (D), n = 4 (E)). For (C), color intensity is proportional to NR activity. Different lowercase letters indicate significant differences determined via Tukey–Kramer tests at $P < 0.05$. ND and NS denote "not detected" and "not significant." FW denotes "fresh weight."

FIGURE 2 Transcriptomic alteration by *AOX1a* deficiency under limited nitrate reduction conditions.

(A–I) One plant from each line (six in total) per plate was grown. Six shoots were pooled as one biological replicate. Shoots from plants 7 h after nitrate supply were subjected to RNA-seq.

518 Numbers indicate the order of RNA-seq experiments. (A) Heat map from a k-means clustering of
519 normalized transcript levels. Magenta and green represent higher and lower expression levels,
520 respectively. (B) Plots of normalized transcript levels in cluster D. Normalized transcript levels
521 of splice variants were averaged for each gene. (C) Venn diagram showing gene number from
522 cluster D and genes significantly upregulated in *aox1a-1 nr* or *aox1a-2 nr* relative to *nr*. (D, E)
523 Enriched terms identified by Metascape (D) and GeneCloud (E) from the 42 genes in (C). (E)
524 shows the number of genes containing the term (left) and the fold enrichment (right). (F–I) Shoot
525 expression of genes upregulated under hypoxia (F), by H_2O_2 (G), by ANAC017 (H), and included
526 in mitochondrial dysfunction stimulon (I) 7h after nitrate supply. Normalized transcript levels of
527 splice variants were averaged for each gene using means from three independent experiments. (J–
528 Q) RT-qPCR analysis of marker genes upregulated under hypoxia (J–M) and by oxidative stress
529 (N–Q) in shoots before and 7 h after nitrate supply. Two plants of each line (eight in total) per
530 plate were grown, and four shoots were pooled as one biological replicate. Data: mean ± SD (n =
531 5). (B, F–Q) Different lowercase letters indicate significant differences determined via Tukey–
532 Kramer tests at $P < 0.05$.
533
534 **FIGURE 3** Effects of *AOX1a* deficiency on gene expression of type II NADP(H) dehydrogenases
535 and uncoupling proteins under limited nitrate reduction conditions.
536 (A) Transcriptional changes in genes encoding type II NADP(H) dehydrogenases (*NDA1/2*,
537 *NDB1/2/4*, *NDC1*), uncoupling proteins (*UCP1/2/3*), and *CI76* encoding the complex I 76-kD
538 subunit in plant shoots 7h after nitrate supply. Transcriptional changes are represented as log2
539 fold change ratios against Col-0 based on the RPM (reads per million mapped reads) from the
540 RNA-seq. Red and blue represent up- (>2-fold) and downregulation (<0.5 fold), respectively.
541 *NDB3* was removed due to low expression. (B,C) Relative transcript levels of *NDB2* (B) and
542 *NDA2* (C) in plant shoots before and 7 h after nitrate supply. Data: mean ± SD (n = 5). Different
543 lowercase letters indicate significant differences determined via Tukey–Kramer tests at $P < 0.05$.

544

545 **FIGURE 4** Effects of *AOX1a* deficiency on shoot growth under limited nitrate reduction
546 conditions.

547 (A, B) Shoot fresh weight (A) and rosette diameter (B) of plants 6 days after nitrate supply. One
548 plant of each line (four in total) per plate were grown and one shoot was pooled as one biological
549 replicate. (C–E) Shoot appearance of 24-day-old plants (C) and shoot fresh weights of 14-day-
550 old (D) and 24-day-old (E) plants grown in pots containing nutrient-rich soil. Data: mean ± SD
551 (n = 17 (A, B), n = 18 (D), n = 7 (E)). Different lowercase letters indicate significant differences
552 determined via Tukey–Kramer tests at $P < 0.05$.

Figure 1

A

Procedure for transfer experiment

	Condition 1 (preculture) →	Condition 2 (preculture) →	Condition 3 (NO_3^- supply)
Duration	18 days	24 hours	0, 2, 4, 7, 24 hours or 6 days
N source	5 mM NH_4^+	No nitrogen	19.7 mM NO_3^- & 10.3 mM NH_4^+
pH	6.7	5.7	5.7
PPFD	30 µmol m^{-2} s^{-1}	30 µmol m^{-2} s^{-1}	150-200 µmol m^{-2} s^{-1}

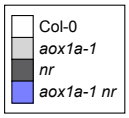

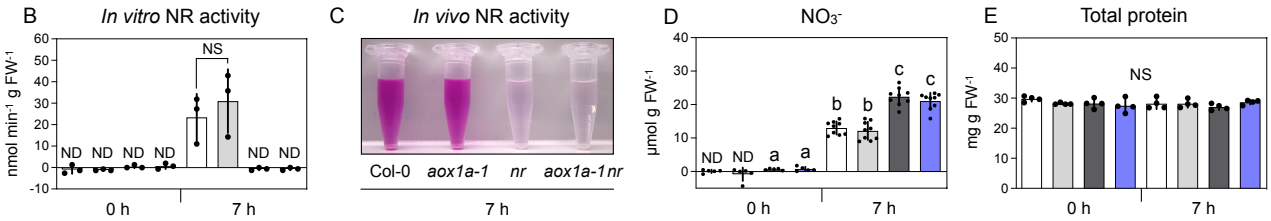

Figure 2

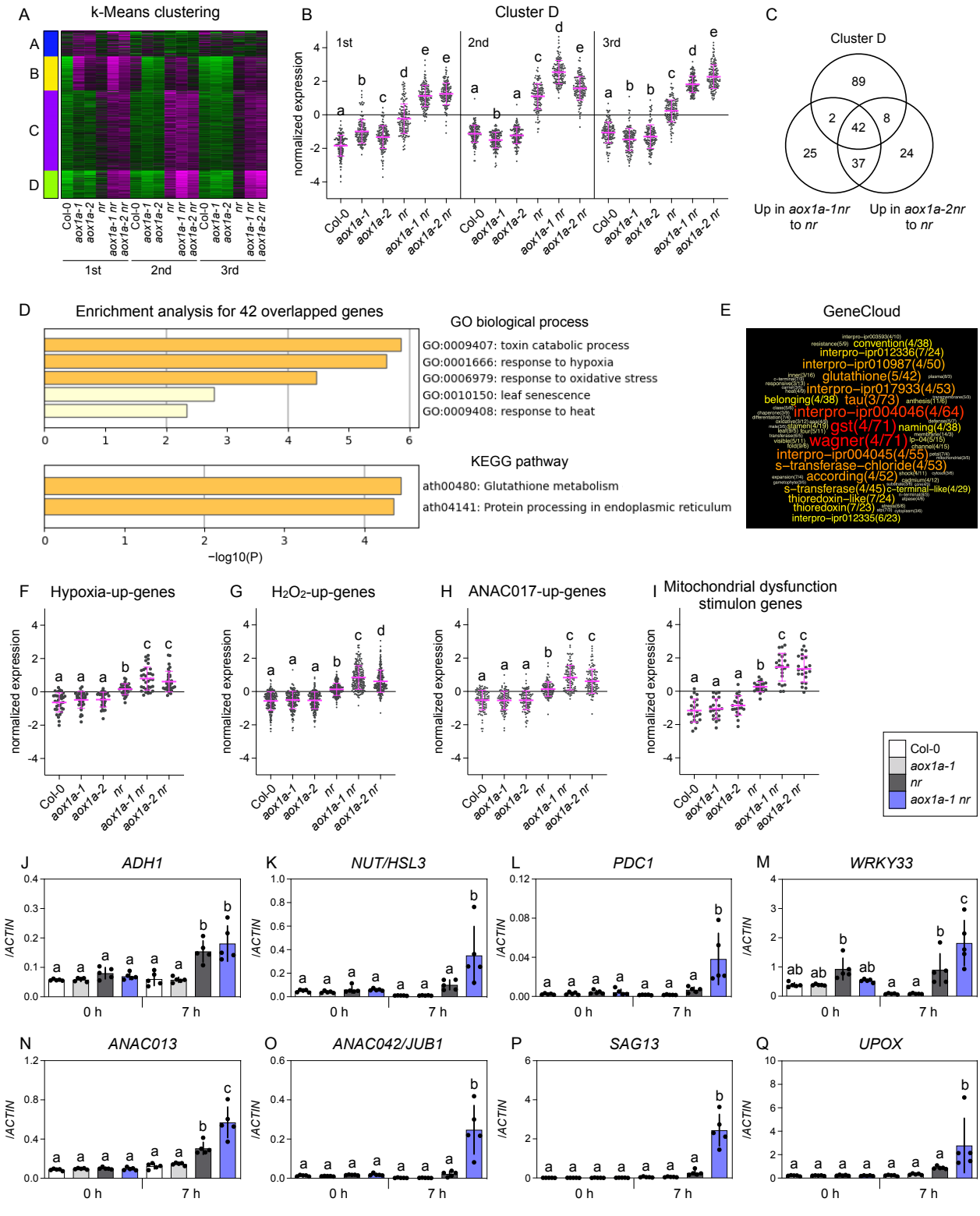
A
k-Means clustering
B
Cluster D
1st
2nd
3rd
normalized expression
C
Cluster D
89
2
8
42
25
24
37
Up in aox1a-1nr to nr
Up in aox1a-2nr to nr
D
Enrichment analysis for 42 overlapped genes
GO biological process
GO:0009407: toxin catabolic process
GO:0001666: response to hypoxia
GO:0006979: response to oxidative stress
GO:0010150: leaf senescence
GO:0009408: response to heat
KEGG pathway
ath00480: Glutathione metabolism
ath04141: Protein processing in endoplasmic reticulum
−log10(P)
E
GeneCloud
convention(4/38)
interpro−ipr012336(7/24)
interpro−ipr010987(4/50)
glutathione(5/42)
interpro−ipr017933(4/53)
belonging(4/38)
tau(3/73)
interpro−ipr004046(4/64)
gst(4/71)
naming(4/38)
wagner(4/71)
interpro−ipr004045(4/55)
s−transferase−chloride(4/53)
according(4/52)
s−transferase(4/45)
c−terminal−like(4/29)
thioredoxin−like(7/24)
thioredoxin(7/23)
interpro−ipr012335(6/23)
F
Hypoxia-up-genes
G
H2O2-up-genes
H
ANAC017-up-genes
I
Mitochondrial dysfunction stimulon genes
Col-0
aox1a-1
aox1a-2
nr
aox1a-1 nr
aox1a-2 nr
J
ADH1
K
NUT/HSL3
L
PDC1
M
WRKY33
N
ANAC013
O
ANAC042/JUB1
P
SAG13
Q
UPOX
/ACTIN
0 h
7 h

Figure 3

A

Transcriptional changes (log2 fold change)

	aox1a-1			*aox1a-2*			*nr*			*aox1a-1 nr*			*aox1a-2 nr*		
Gene	1st	2nd	3rd	1st	2nd	3rd	1st	2nd	3rd	1st	2nd	3rd	1st	2nd	3rd
NDA1	-0.2	-0.4	0.0	-0.2	0.1	-0.1	-0.1	-0.2	0.1	0.4	0.2	0.4	0.2	0.3	0.6
NDA2	-0.2	0.4	-1.1	-0.2	-0.2	-0.5	-0.0	0.8	-0.2	0.7	2.5	1.2	0.6	1.1	1.6
NDC1	0.0	0.2	-0.0	-0.1	0.3	0.0	0.0	0.1	0.1	-0.1	-0.0	0.0	0.1	0.1	-0.2
NDB1	-0.1	-0.0	-0.1	-0.0	-0.1	0.0	0.1	0.2	-0.1	-0.1	-0.1	0.1	-0.1	-0.0	-0.3
NDB2	0.4	-0.1	-0.5	0.4	0.1	-0.1	0.9	1.2	0.4	1.9	2.4	1.7	2.4	2.0	1.8
NDB4	-1.6	1.0	0.3	0.1	-	2.7	-1.0	1.9	1.6	0.3	3.3	2.7	-0.6	1.7	2.6
UCP1	-0.1	0.3	0.3	-0.1	0.1	0.2	-0.2	-0.1	0.1	-0.1	0.1	0.1	-0.1	0.1	0.3
UCP2	-0.1	-0.0	-0.3	-0.1	-0.1	0.1	-0.2	-0.2	0.1	-0.2	-0.3	-0.1	-0.2	-0.3	-0.2
UCP3	-0.4	0.2	-0.1	-0.4	0.3	0.0	-0.6	0.4	0.1	-0.7	-0.2	0.0	-0.4	0.2	-0.5
CI76	-0.1	0.1	-0.2	0.0	-0.0	-0.1	-0.1	0.1	-0.1	-0.0	-0.0	-0.2	-0.0	-0.0	-0.3

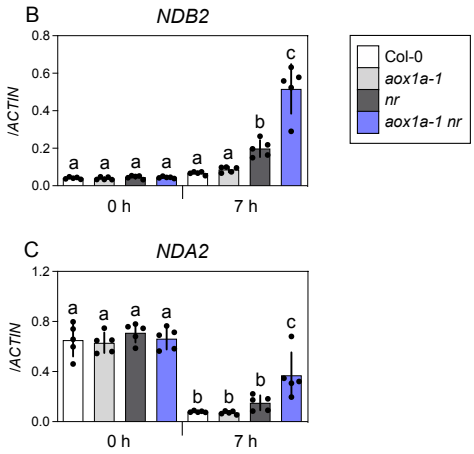

Figure 4

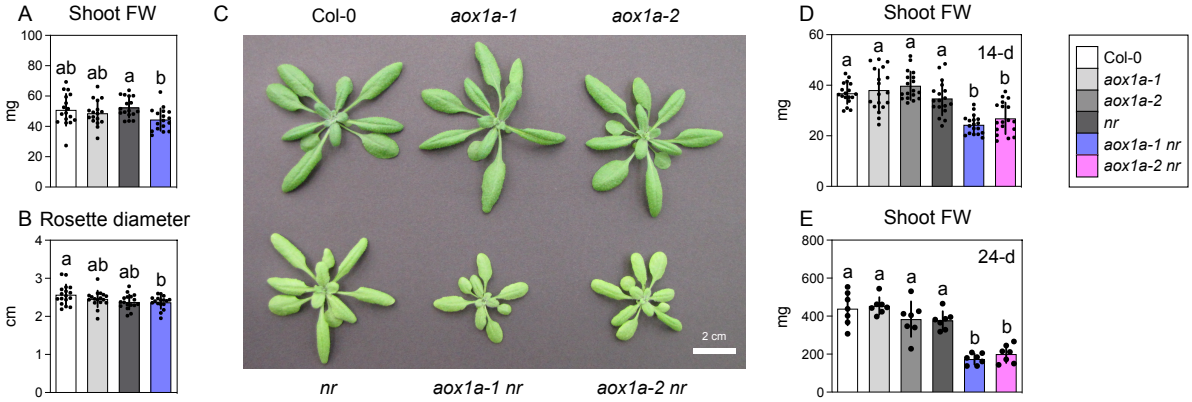
A
Shoot FW
mg
ab
ab
a
b
B
Rosette diameter
cm
a
ab
ab
b
C
Col-0
aox1a-1
aox1a-2
nr
aox1a-1 nr
aox1a-2 nr
2 cm
D
Shoot FW
14-d
mg
E
Shoot FW
24-d
mg
Col-0
aox1a-1
aox1a-2
nr
aox1a-1 nr
aox1a-2 nr